

Military Technical College
Kobry El-Kobba,
Cairo, Egypt



11-th International Conference
on Aerospace Sciences &
Aviation Technology

INVESTIGATION OF MODE SCATTERING BY HARD STRIPS IN LINED DUCTS USING COLLOCATION

Elnady* T.

ABSTRACT

When mounting acoustic liners inside the inlet duct of aircraft jet engines, hard strips exist in-between liner sections in order to hold them in place. It has been generally acknowledged, from experiments, that the existence of hard strips inside lined ducts affects the attenuation behaviour of the duct. The acoustic energy is scattered and rearranged among different modes so that it might be transferred into modes which are less attenuated by the liner. Moreover, cut-off modes may scatter into cut-on modes. In this paper, flow is included in the locally reacting liner case, which is more interesting to the aeronautics applications. Moreover, the duct is made finite and connected to two semi-infinite hard inlet and outlet ducts. By using mode matching, it is possible to input any mode at the inlet side and to study the modes on the outlet side. Comparisons are made between different hard strip cases and the splice-less liner case.

KEY WORDS

Acoustic liners, hard strips, Jet engine noise.

INTRODUCTION

One of the main sources of noise in aircraft is the engine. Many recent studies on noise reduction involve the use of acoustically absorbent material in the air and gas flow ducting of the engine. Although the lined wall may have been designed to be uniform, a variation in admittance may result from the mounting techniques, which can make the existence of hard strips inevitable, to hold the liners in place.

Watson¹ developed Finite Element Methods to analyze sound attenuation in ducts with a peripherally variable liner. For a finite duct with no flow, he showed that the attenuation

* Assistant Professor, Sound and Vibration Lab., Faculty of Engineering, Ain Shams University, Cairo, Egypt.

rate near the frequency of maximum attenuation drops significantly if a small portion of a peripheral liner is removed.

From the in-flight circumferential modal spectra of the Rolls-Royce Tay 650 engine mounted on the Fokker 100 aircraft, Sarin and Rademaker² found that the sound field propagating upstream in the inlet is strongly modulated by hard-walled strips in the lined area, the non-cylindrical geometry of the duct and the non-axisymmetric flow velocity distribution. In order to study the effect of the modulation of the acoustic field by the hard-walled strips separately, an experimental program in the NLR spinning mode synthesizer was carried out³.

Regan & Eaton developed a FE model^{4,5} and used it to analyze a finite duct lined with locally reacting liner with different number of hard strips of different widths. They demonstrated that the transmitted modal spectrum can be significantly modulated by the presence of hard strips, but for the frequency range considered ($ka < 10$), the overall transmitted power is not significantly affected.

The solution of the eigenvalue problem inside a circular duct is simple as long as the duct is axi-symmetric, because the variables are separable, see for example⁶. When the boundary condition varies around the circumference, the property of the field being separable breaks down. Therefore, a more complicated technique has to be used. The most well known method is probably FEM^{4,7}. FEM may, especially for the analysis of higher order modes, be somewhat cumbersome and is thus not ideally suited in an iterative design process. However, there are a number of other methods such as null-field⁸, Rayleigh-Ritz⁹ and collocation¹⁰. The collocation technique has been already tested to handle hard discontinuities in lined ducts and showed good potential¹¹.

Bi *et al.*¹² used the Multimodal Method to solve the problem of sound transmission through circular cylindrical ducts lined with a non-uniform impedance in the absence of flow. The liner impedance was assumed to be piecewise constant along the axis of the duct, and can arbitrary vary along the circumference. First, the Euler and continuity equations are projected over the eigenfunctions of a rigid uniform duct. Mode coupling effects are then explicitly expressed by the inverse Fourier transformation of liner admittance. Second, a scattering matrix is used to express the reflection and transmission coefficients of each axial uniform segment from which a global scattering matrix can be constructed.

The collocation technique was earlier used to calculate the wavenumbers of the modes in an infinite lined duct with hard strips¹¹. The problem is taken a step forward in this paper by considering a duct of a finite length. The field in the lined duct must be linked to the field in the hard ducts before and after the lined section. Mode matching determines how energy is transferred and scattered between modes across the lined section when hard strips exist. The formulation presented here is valid for any cross section with flow, as long as the fields in the three ducts are pre-determined, provided that the liner in the intermediate duct is locally reacting.

THEORETICAL APPROACH

The considered configuration is shown in Fig. 1. A single mode, of any order m and n , is incident at the inlet duct emanating from a sound source, e.g. a rotating fan. The generated wave, Ψ_{1i} , travels towards the lined section and is scattered at $z = 0$ to a reflected, Ψ_{1r} , and transmitted Ψ_{2i} wave. The travelling wave in the lined duct is further scattered at $z = L$ into reflected, Ψ_{2r} , and transmitted waves, Ψ_{3i} . The hard ducts are assumed to be semi-infinite so that no waves are reflected from the other ends. The numbering of the fields is as follows: 1 for the inlet hard duct, 2 for the lined duct and 3 for the outlet hard duct. The letter i refers to the incident wave and the letter r refers to the reflected one. The boundary condition in the lined duct can vary around the circumference to allow the definition of the hard strips.

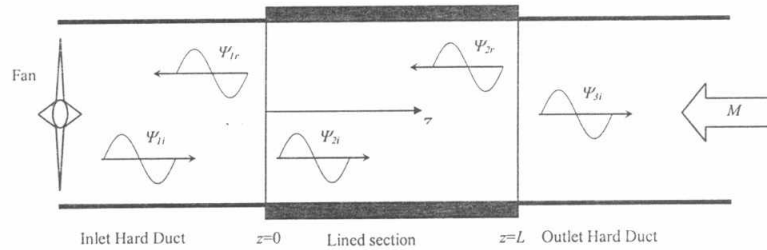


Fig. 1 Incident, reflected and transmitted modes in the calculation domain.

Since the acoustic field is irrotational, the velocity vector can be expressed as a gradient of a certain potential which is a scalar quantity ($u = \nabla \Psi$). It can be easily shown that the convective wave equation can be expressed in terms of the velocity potential. A stationary problem is considered where all the fields and their derivatives are time harmonic with $e^{i\omega t}$. When the direction of the mean flow is in the axial direction, the wave equation reduces to

$$\nabla^2 \Psi - \left(jk + M \frac{\partial}{\partial z} \right)^2 \Psi = 0 \tag{1}$$

where Ψ is the temporal Fourier transform of the velocity potential. The solution to this equation can be considered as a sum of linearly independent acoustic modes, each satisfies the same wave equation and the same boundary conditions.

$$\Psi(r, \theta, z) = \sum_{q=1}^Q b^{(q)} \cdot \psi^{(q)}(r, \theta) \cdot e^{-jk^{(q)}z} \tag{2}$$

where q is the mode number, $b^{(q)}$ is the amplitude of the q^{th} mode, and ψ is the two-dimensional mode shape of the q^{th} mode after separating the z dependence because the duct is now assumed infinite. The modes are arranged in an ascending order according to their cut-on frequency in the corresponding hard wall duct. Equation (1) can

be simplified, for each mode $\Psi_2^{(q)} = \psi_2^{(q)} \cdot e^{-jk_z^{(q)}z}$, using the expansions of the derivative operators to

$$\nabla_{\perp}^2 \psi^{(q)} + (k_{\perp}^{(q)})^2 \cdot \psi^{(q)} = 0 \quad (3)$$

where the transversal wave number, $k_{\perp}^{(q)}$, is given by

$$(k_{\perp}^{(q)})^2 = k^2 - 2kMk_z^{(q)} - (1 - M^2)(k_z^{(q)})^2 \quad (4)$$

The terminology of the transversal wavenumber, k_{\perp} , is used here instead of the radial wavenumber, k_r , because in spite of the fact that the duct is circular, the boundary condition is not axi-symmetric. Therefore, the field is not separable in the two-dimensional plane perpendicular to the duct axis. The transversal and axial wavenumbers are scaled as $k := ka$ and consequently, the distances are scaled as $x := x/a$, where a is the duct radius.

A. The acoustic field in a lined duct using collocation

For the two-dimensional field, it is solved by using the point-matching or collocation method¹¹. The field is approximated by finite expansions in the polar eigenfunctions

$$\psi_2^{(q)} = \sum_{w=0}^W J_w(k_{\perp}^{(q)}r) (A_w^{(q)} \cos w\theta + B_w^{(q)} \sin w\theta) \quad (5)$$

The acoustic field in the lined duct is now represented using Eqs. (2) and (5) by

$$\Psi_2^{(q)} = \left[A_0 J_0(k_{\perp}^{(q)}r) + \sum_{w=1}^W J_w(k_{\perp}^{(q)}r) (A_w^{(q)} \cos w\theta + B_w^{(q)} \sin w\theta) \right] \cdot e^{-jk_z^{(q)}z} \quad (6)$$

where the first term is treated separately for convenience. The transversal and axial wavenumbers are related by equation (4). The boundary condition at the duct wall ($r = 1$) is based on the assumption that the lining is locally reacting. To the mean flow, the duct wall is hard, but for the acoustic field the duct is lined with an impedance boundary condition. The following simplified equation is obtained for the boundary condition

$$\left[\nabla \psi \cdot n \Big|_{r=b} + \frac{jA}{k} (k_{\perp}^2 + k_{z2}^2) \psi \right] \cdot e^{-jk_z^{(q)}z} = 0 \quad (7)$$

where n is the normal vector to the liner surface and directed into the wall and A is the acoustic admittance at the wall (the reciprocal of the impedance). This is an acceptable assumption when plug flow is assumed. This yields the following expression

$$A_0 \left[k_{\perp} J_0'(k_{\perp} a_i) + \frac{jA}{k} (k_{\perp}^2 + k_{z2}^2) \cdot J_0(k_{\perp} a_i) \right] + \sum_{w=1}^W A_w \left[\left(k_{\perp} J_w'(k_{\perp} a_i) + \frac{jA}{k} (k_{\perp}^2 + k_{z2}^2) \cdot J_w(k_{\perp} a_i) \right) \cos(w\theta_i) \right] + \sum_{w=1}^W B_w \left[\left(k_{\perp} J_w'(k_{\perp} a_i) + \frac{jA}{k} (k_{\perp}^2 + k_{z2}^2) \cdot J_w(k_{\perp} a_i) \right) \sin(w\theta_i) \right] = 0 \quad (8)$$

Equation (8) represents a set of finite number of simultaneous equations and can be written in matrix form. The system matrix has the dimension of $(P \times P)$. The collocation points are defined by $a_i = a(\varphi_i)$ where $i = 1, 2, \dots, P$ and P must be set to be equal to $(2W+1)$ in order to equate the number of equations and the number of unknowns. To avoid non-trivial solutions, the rows of the system matrix must be linearly independent; in other words, its determinant must be equal to zero constituting the dispersion relation for the eigenmodes of the lined duct. The wavenumbers for the lined duct are obtained using the secant iteration method starting from the wavenumbers solutions for a circular hard duct. The secant method is able to predict the value of a function based on two previous values. The iteration is performed in the complex plane of the axial wavenumber in order to have physical insight into the solution concerning left and right propagating waves. The first two values for the admittance stepping are the wavenumber for the hard duct and the same wavenumber but with a slightly perturbed imaginary part. The relation between k_z and k_{\perp} in equation (4) was combined with eigenvalue equation to have only one independent variable. First, the admittance is increased with sufficiently small steps from zero to its final value, and then the Mach number is increased with the same step to its final value. It is very important to choose sufficiently small steps to reach the correct solution without losing trace of the wavenumber or jumping to an adjacent one. In order to decrease the number of steps, a growing step can be used because the start of the trajectory is very critical. Once the wavenumbers are known, the modal amplitude coefficients can be calculated for each mode. The total acoustic field in the lined duct is the sum of incident and reflected waves

$$\Psi_2 = \sum_{q=1}^Q b_+^{(q)} \psi_2^{(q)} e^{-jk_z^{(q)} z} + \sum_{q=1}^Q b_-^{(q)} \psi_2^{(q)} e^{jk_z^{(q)} (z-L)} \quad (9)$$

In order to get stable matrices and enhance their manipulation, it is better to refer each mode to the plane at which it is generated. For example, the right propagating modes in the lined section are generated at $z = 0$, and the left propagating modes in the lined section are generated at $z = L$.

B. Fields in a circular duct with uniform boundary condition

For a circular duct with a uniform circumferential boundary condition either lined or hard, the duct becomes axi-symmetric so that the two-dimensional field is separable

$$\psi^{(q)} = J_m(k_r^{(q)} r) \cdot [A_m^{(q)} \cos(m\theta) + B_m^{(q)} \sin(m\theta)] \quad (10)$$

The modes are numbered here in an ascending order according to their cut-on frequency. Each mode is divided into two parts treated separately; each part consists of one term. This is to give A_m and B_m the freedom to have any value. If the duct is lined with a uniform impedance boundary condition, equation (10) can be substituted in the boundary condition to give a simpler eigenvalue relation to calculate the radial wavenumbers in the circular duct

$$k_{12}^{(q)} \frac{J'_m(k_{12}^{(q)})}{J_m(k_{12}^{(q)})} + j \frac{A}{k} \left[(k_{12}^{(q)})^2 + (k_{z2}^{(q)})^2 \right] = 0 \quad (11)$$

where the axial wavenumber, $k_z^{(q)}$, is related to the transversal wavenumber, $k_{\perp}^{(q)}$, by the dispersion relation in equation (4). In the hard ducts before and after the lined section, the boundary condition is different and the normal velocity at the wall is zero, i.e. $A = 0$

$$\nabla \Psi_1 \cdot n|_{r=a} = 0 \quad (12)$$

which gives the following eigenvalue equation

$$J'_m(k, r) = 0 \quad (13)$$

and the axial wavenumbers are calculated from

$$k_{z2}^{(q)} = \frac{k}{1-M^2} \left[-M \pm \sqrt{1 - (1-M^2) \frac{(k_{12}^{(q)})^2}{k^2}} \right] \quad (14)$$

Note that there are two values of the axial wavenumber for each radial wavenumber corresponding to the propagation direction. An acoustic energy argument can be used to show that the positive sign in equation (14) corresponds to the acoustic power transmitted in the positive z-direction and the negative sign corresponds to the acoustic power transmitted in the negative z-direction¹⁵. This is only true for the cut-on modes and vice versa for the cut-off modes. Every solution of the eigenvalue equation corresponds to a propagating mode. The acoustic field is a summation of all the propagating modes

$$\Psi_1 = a_s^{(q_s)} \psi_1^{(q_s)} e^{-jk_{z1}^{(q_s)} z} + \sum_{q=1}^Q a^{(q)} \psi_1^{(q)} e^{jk_{z1}^{(q)} z} \quad (15)$$

Similarly, the field in the outlet duct can be represented as

$$\Psi_3 = \sum_{q=1}^Q c_s^{(q)} \psi_3^{(q)} e^{-jk_{z3}^{(q)} (z-L)} \quad (16)$$

D. Mode Matching

Mode matching is a well-known technique which is used to determine how energy is transferred and scattered between modes at an interface where there is a discontinuity in either duct dimensions or transversal boundary conditions. Cummings & Chang¹⁶ used mode matching to calculate the sound attenuation of a circular dissipative silencer with flow. Glav¹⁷ used it to calculate the transfer matrix for a dissipative silencer of arbitrary cross section but with no mean flow. Peat¹⁸ calculated the transfer matrix for an absorption circular silencer element with flow. The aforementioned studies were done for silencers in automotive applications; therefore, the used liner was non-locally

reacting. There was sound propagation inside the liner but the mean flow in the liner is neglected compared to that in the main duct. Peat¹⁹ also used mode matching to determine equivalent acoustic impedance at the junction of an extended inlet or outlet inside a circular silencer to be able to calculate its transfer matrix. Lansing & Zorumski²⁰ used the technique to evaluate the effect of axially changing the wall admittance of a circular lined duct with no flow in order to evaluate the effect on the transmitted power.

The formulation presented here is valid for any cross section with flow, as long as the fields in the three ducts are pre-determined, provided that the liner in the intermediate duct is locally reacting. According to the theory of relative convergence¹⁷, the number of considered modes in both ducts must be equal as long as their areas are equal. The boundary conditions at the interface between any two adjacent ducts implies the continuity of acoustic pressure and axial velocity at $z = 0$ and $z = L$. By substituting the acoustic fields from equations (9), (15) and (16) in these boundary conditions, and multiplying by the mode shapes in the hard duct $\psi_1^{(u)}$, where $u = 1..Q$, then integrate over the cross-section. After careful manipulation, the axial boundary conditions can be shown to yield the following set of independent equations

$$\sum_{q=1}^{Q_0} a_-^{(q)} \Lambda_{11}^{qu} - \sum_{q=1}^{Q_0} b_+^{(q)} \Lambda_{211}^{qu} - \sum_{q=1}^{Q_0} b_-^{(q)} \Lambda_{2r1}^{qu} e^{-jk_z^{(q)}L} = -a_+^{(q_0)} \Lambda_{11}^{q_0u} \quad (17)$$

$$\sum_{q=1}^{Q_0} c_+^{(q)} \Lambda_{11}^{qu} - \sum_{q=1}^{Q_0} b_+^{(q)} \Lambda_{211}^{qu} e^{-jk_z^{(q)}L} - \sum_{q=1}^{Q_0} b_-^{(q)} \Lambda_{2r1}^{qu} = 0 \quad (18)$$

$$-\sum_{q=1}^{Q_0} a_-^{(q)} \Lambda_{11}^{qu} k_{z1r}^{(q)} - \sum_{q=1}^{Q_0} b_+^{(q)} \Lambda_{211}^{qu} k_{z2i}^{(q)} + \sum_{q=1}^{Q_0} b_-^{(q)} \Lambda_{2r1}^{qu} k_{z2r}^{(q)} e^{-jk_z^{(q)}L} = -a_+^{(q_0)} \Lambda_{11}^{q_0u} k_{z1r}^{(q_0)} \quad (19)$$

$$\sum_{q=1}^{Q_0} c_+^{(q)} \Lambda_{11}^{qu} k_{z1i}^{(q)} - \sum_{q=1}^{Q_0} b_+^{(q)} \Lambda_{211}^{qu} k_{z2i}^{(q)} e^{-jk_z^{(q)}L} + \sum_{q=1}^{Q_0} b_-^{(q)} \Lambda_{2r1}^{qu} k_{z2r}^{(q)} = 0 \quad (20)$$

where q_0 is the order of the incident mode, and Λ is defined as

$$\Lambda_{pv}^{qu} = \int_0^{2\pi} \int_0^1 \psi_p^{(q)} \psi_v^{(u)} r dr d\theta \quad (21)$$

Equations (17) to (20) are written in matrix form. All unknown modal amplitudes are calculated by solving the above system of linear equations in $4Q$ unknowns ($a_-^{(q)}$, $c_+^{(q)}$, $b_+^{(q)}$, $b_-^{(q)}$). The amplitude of the input mode, a_+ , is normalized to 1 and all the other modal amplitudes are calculated with reference to it. To achieve the full advantage and speed of the mode-matching method, all integrals are evaluated analytically. One advantage of choosing the eignfunctions in the hard duct as the basis function is that they are orthogonal; a property which reduces the matrix size enormously. All Λ s are independent double integrals in r and θ that can be divided into two single integrals evaluated separately.

RESULTS AND DISCUSSION

A. Validation with simple configurations

A series of simple duct tests were examined to validate the formulation and the computer code. All the test cases will be compared with the Finite Element calculations presented in reference 5. In the first case, the intermediate duct was completely hard as the inlet and outlet ducts. The second test case was a semi-infinite hard walled duct with uniform flow and one end closed by an acoustically hard termination. The third test case was more appropriate where a liner of finite admittance is placed at the walls of the intermediate duct. The duct was circular of 0.2 m radius, and the length of the lined section was 0.4 m. Four test cases were considered and their parameters are listed in Table 1. Computed values for the transmitted normalized modal amplitudes $|c_+|/|a_+|$ of the incident mode for each case are listed in the last two columns. Two values are shown, one calculated by mode matching and the other calculated by FEM from reference 5. It can be seen that there is close agreement between the mode matching and Finite Element calculations. In Fig. 2, the field results are plotted as contours of the amplitude of the computed complex pressure for case number 3 in Table 1.

Table 1 Different parameters used for different cases, and comparison of the calculated transmitted, normalized modal amplitudes of the incident mode for each case.

Case	z	M	Incident mode	ka	Mode matching	FEM
1	(1,-2)	0	(0,0)	1.5	0.6499	0.65
2	(1,-2)	-0.3	(0,0)	1.5	0.1717	0.17
3	(2,-1)	-0.3	(0,2)	7.4	0.1323	0.13
4	(3,0)	-0.3	(5,0)	7.4	0.0118	0.012

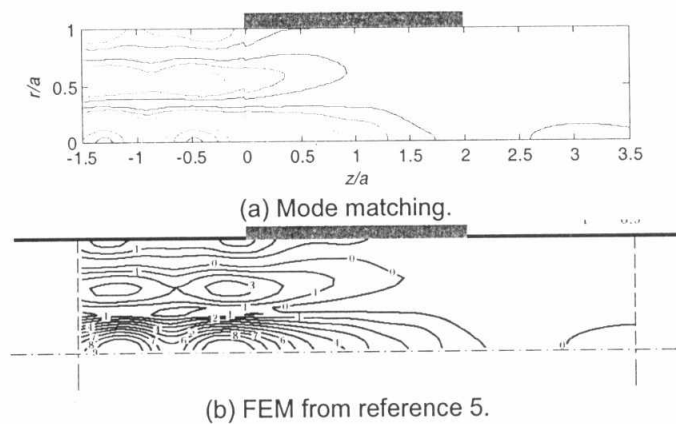


Fig. 2 Calculations of amplitude pressure contours for incident mode (0, 2), impedance (2, -1) in the intermediate duct, $M = -0.3$ and $ka = 7.4$, $L/a = 2$.

B. Validation with hard strips

The next step is to apply the combined collocation and mode matching code to the case with hard strips and compare the results with the Finite Element predictions. The configuration in reference 5 will be considered which contains two hard strips. The strips are diametrically opposite to each other and each extends circumferentially over an angle of 0.75 rad. The duct has a diameter of 0.2 m as before and a lined section of 0.4 m. This corresponds to configuration 4 in reference 5, see Fig. 3. Without flow, the non-dimensional impedance was specified in reference 5 as follows: a resistance of 1.5, a mass reactance of 0.01k and a cavity reactance of $-\cot(0.016k)$.

$$z = 1.5 + j(0.01k - \cot(0.016k)) \tag{22}$$

To investigate the effect of the liner splices, a single incident mode is injected and the resulting transmitted modal spectrum is calculated. This spectrum is compared with the transmitted field produced by a uniform homogeneous liner modelled under the same conditions. The transmitted modal amplitudes are normalized with respect to the amplitude of the single incident mode.

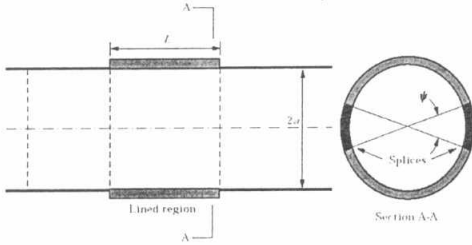


Fig. 3 The lined section with two splices (Configuration 4 in reference 5).

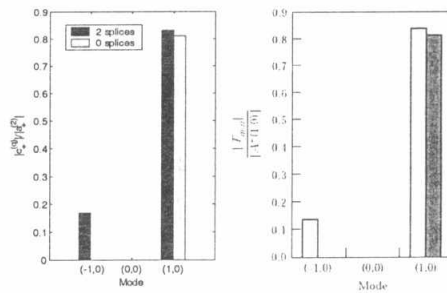


Fig. 4 Comparison of the scattering spectra. $M = 0$, $ka = 2.2$, 2 splices (.75 rad), and incident mode (1, 0).

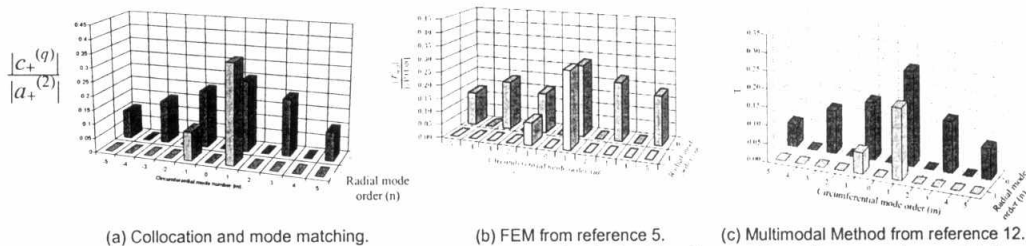
The first set of calculations is performed at 600 Hz, which corresponds to a ka value of 2.217. At this frequency, only modes (0, 0), (1, 0), and (-1,0) are cut-on, so that the effect of the scattering on a single mode should be easy to isolate. Mode (1, 0) is injected in the inlet duct then both the uniform and spliced configurations are solved and compared in Fig. 4. In the same figure, they are also compared with the finite element calculations presented in reference 5. For an axi-symmetric duct, only the incident mode and other modes having the same circumferential order m appear in the transmitted spectrum. This is because there is no mechanism to generate modes of other circumferential orders. Only cut-on modes are presented in the figures because scattered cut-off modes have no importance as they do not carry any energy. For the spliced case, two changes occur. The transmitted amplitude for the spliced arrangement is larger than for the uniform liner, which is expected since the latter has a larger lined surface area. Scattering effects cause modes of other circumferential orders to be excited and therefore mode (-1, 0) is excited and transmitted because it is also cut-on.

By analogy to the rotor-stator interaction theory²², the circumferential order of the modes excited by scattering can be specified by

$$m = m_i \pm \beta \cdot N \quad \beta = 0, 1, 2, \dots \tag{23}$$

where m_i is the circumferential order of the injected incident mode and N is the number of splices. The second test case was conducted at 1830 Hz, corresponding to a wavenumber of $ka = 6.8$. This frequency was chosen to demonstrate the behaviour described by equation (23) over a broader range of circumferential mode orders. In this case, all zero-order radial modes of circumferential order less than six are cut-on, in addition to first-order radial modes of circumferential order less than three (a total of 16 modes). The incident mode was chosen to be (1, 0). When the same mode was injected towards a liner with two strips, modes with circumferential order $-5, -3, -1, 3, 5$, which are cut on, were also excited. This is illustrated in Fig. 5, where the scattered spectrum of the combined collocation and mode matching technique is compared to that calculated by Finite Elements in reference 5 and the Multimodal Method in reference 12. Although there are some discrepancies between the three methods in the exact values of the amplitudes of the scattered waves, the general shape looks similar for the three methods.

The amplitudes of the scattered modes do not give much information about the transmitted sound energy across the lined section because each mode has its own decay rate and ability to carry energy. Therefore, it is important to compare the transmitted sound power with and without hard strips. Fig. 6 compares the propagating sound power for the previous duct case at $ka = 6.8$, and 2 strips (0.75 rad each). As expected, the transmitted power increases slightly when hard strips are present.



(a) Collocation and mode matching. (b) FEM from reference 5. (c) Multimodal Method from reference 12.
 Fig. 5 Comparison of the scattering spectra calculated by the collocation mode matching technique, FEM from reference 5, and the multimodal method from reference 12. $M = 0$, $ka = 6.8$, 2 splices (.75 rad), and incident mode (1, 0).

CONCLUSIONS

It is inevitable to have hard strips between liner segments in the inlet of aircraft jet engines. It has been found that these strips scatter the modal energy among different modes. An analytical formulation is presented here to calculate the scattered transmitted modal spectrum when a single mode is input from one side of the lined duct. The

wavenumbers in the lined section are found by collocation, and then the modes are matched at the duct interface. The formulation is valid for any cross section with flow provided that the liner in the intermediate duct is locally reacting.

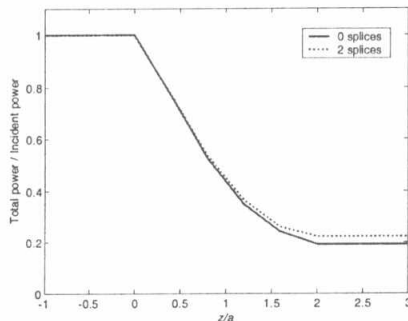


Fig. 6 The propagating sound power across the lined section with and without splices.

ACKNOWLEDGEMENT

Financial support from the NFFP (National Flight Research Program) is gratefully acknowledged.

REFERENCES

1. Watson, W., "A Finite Element Simulation of Sound Attenuation in a Finite Duct with a Peripherally Variable Liner," NASA TM-74080, 1977.
2. Sarin, S., and Rademaker, E., "In-Flight Acoustic Mode Measurements in the Turbofan Engine Inlet of Fokker 100 Aircraft," AIAA Paper 93-4414, 1993.
3. Rademaker, E., Sarin, S., and Parente, C., "Experimental Investigation on the Influence of Liner Non-Uniformities on Prevailing Modes," AIAA Paper 96-1682, 1996.
4. Regan, B., and Eaton, J., "Finite Element Investigation of the Influence of Liner Splices on Duct Modes," AIAA Paper 98-2313, 1998.
5. Regan, B., and Eaton, J., "Modelling the Influence of Acoustic Liner Non-Uniformities on Duct Modes," *Journal of Sound and Vibration*, Vol. 219, No. 5, 1999, pp. 859-879.
6. Eversman, W., "Theoretical Models for Duct Acoustic Propagation and Radiation," *Aeroacoustics of flight vehicles, Theory and Practice*, Acoustical Society of America, New York, 1995.
7. Astley, J., and Cummings, A., "A Finite Element Scheme for Attenuation in Ducts Lined with Porous Material: Comparison with Experiments," *Journal of Sound and Vibration*, Vol. 116, No. 2, 1987, pp. 239-263.

8. Glav, R., "The Null-Field Approach to Dissipative Silencers of Arbitrary Cross Section," *Journal of Sound and Vibration*, Vol. 189, No. 4, 1996, pp. 489-509.
 9. Cummings, A., "Sound Absorbing Ducts," *Proceedings of the 2nd International Congress on Recent Developments in Air- and Structure-Borne Sound and Vibration*, Auburn, USA, 1992, pp. 689-696.
 10. Dahlquist, G., and Bjork, A., *Numerical Methods*, Prentice-Hall, New Jersey, 1974.
 11. Elnady, T., and Bodén, H., "Hard Strips in Lined Ducts", AIAA 2001-2444, May 2001.
 12. Bi, W., Pagneux, V., Lafarge, D., and Aurégan, Y., "Sound Propagation in Non-Uniform Lined Duct by the Multimodal Method," *Proceedings of the 10th International Congress on Sound and Vibration*, Stockholm, Sweden, July 2003.
 13. Myers, M., "On the Acoustic Boundary Condition in the Presence of Flow," *Journal of Sound and Vibration*, Vol. 71, No. 3, 1980, pp. 429-434.
 14. Aurégan, Y., Starobinski, R., and Pagneux, V., "Influence of Grazing Flow and Dissipation Effects on the Acoustic Boundary Conditions at a Lined Wall", *Journal of the Acoustical Society of America*, Vol. 109, No. 1, 2001, pp. 59-64.
 15. Eversman, W., "Energy Flow Criteria for Acoustic Propagation in Ducts with Flow," *Journal of the Acoustical Society of America*, Vol. 49, No. 6, 1971, pp. 1717-1721.
 16. Cummings, A., and Chang, I.-J., "Sound Attenuation of a Finite Length Dissipative Flow Duct Silencer with Internal Mean Flow in the Absorbent," *Journal of Sound and Vibration*, Vol. 127, No. 1, 1988, pp. 1-17.
 17. Glav, R., "The Transfer Matrix for a Dissipative Silencer of Arbitrary Cross Section," *Journal of Sound and Vibration*, Vol. 236, No. 4, 2000, pp. 575-594.
 18. Peat, K., "A Transfer Matrix for an Absorption Silencer Element," *Journal of Sound and Vibration*, Vol. 146, No. 2, 1991, pp. 353-360.
 19. Peat, K., "The Acoustical Impedance at the Junction of an Extended Inlet or Outlet Duct," *Journal of Sound and Vibration*, Vol. 150, No. 1, 1991, pp. 101-110.
 20. Lansing, D., Zorumski, W., "Effects of Wall Admittance Changes on Duct Transmission and Radiation of Sound," *Journal of Sound and Vibration*, Vol. 27, No. 1, 1973, pp. 85-100.
 21. Rienstra, S., and Hirschberg, A., "An Introduction to Acoustics", Eindhoven University of Technology, The Netherlands, IWDE 92-06, 2001.
 22. Tyler, J., and Sofrin, T., "Axial Flow Compressor Noise Studies," *SAE Transactions*, Vol. 70, 1962, pp. 309-332.
-